Nontrivial Tuning of the Hydrogen–Binding Energy to Fullerenes with Endohedral Metal Dopants

ARTICLE *in* THE JOURNAL OF PHYSICAL CHEMISTRY C · SEPTEMBER 2007

Impact Factor: 4.77 · DOI: 10.1021/jp073482a

Nontrivial Tuning of the Hydrogen-Binding Energy to Fullerenes with Endohedral Metal Dopants

Yufeng Zhao,*,† Michael J. Heben,† Anne C. Dillon,† Lin J. Simpson,† Jeff L. Blackburn,† Harry C. Dorn,‡ and Shengbai B. Zhang†

National Renewable Energy Laboratory, 1617 Cole Blvd, Golden, Colorado 80401, and Department of Chemistry, Virginia Polytechnic Institute and State University, Blacksburg, Virginia 24061

Received: May 7, 2007; In Final Form: June 21, 2007

We report a first-principle study of the tunable hydrogenation of endohedral metallofullerenes M@C_{60} and M_2@C_{60}, where M = Li, Be, Mg, Ca, Al, and Sc. The interaction between the encapsulated metal atoms and the C_{60} cage leads to a tuning of the hydrogen binding in a desired manner as the hydrogenation proceeds. At lower H densities, when H atoms are too strongly bound to pure C_{60}, the endohedral dopants weaken the binding. The dopants also enhance the hydrogen-binding energy at higher coverages and enable the degree of hydrogenation to be substantially increased relative to that available with empty-cage C_{60}. Overall, the encapsulated metals increase the capacity and improve the energy efficiency for hydrogen storage. We identify materials capable of storing 6.1 wt % hydrogen and elucidate a subtle interplay between reactivity and structure which will be important for designing the next-generation hydrogen-storage materials.

1. Introduction

The internal empty cavity of fullerene cages inspires endohedral doping for fine-tuning the chemical, optical, and redox properties of fullerenes.[1] Since the beginning of fullerene chemistry, endohedral fullerenes[2,3] have attracted interest because the encapsulated atoms (usually metals) can impart unique physical and chemical properties.[3−6] Also, the metal can readily donate charge to the cage, and this effect stabilizes certain empty-cage fullerenes other than C_{60}. For example, scandium, calcium, other metals, and trimetallic nitride clusters have been encapsulated to yield various types of endohedral metallofullerenes.[7−14]

Hydrogenation of fullerenes has been investigated to probe fullerene reactivity[1,15−19] and for possible use in hydrogen-storage applications.[20−26] Hydrogen storage through hydrogenation of the pure empty-cage fullerene is hindered by several problems. A first problem is insufficient hydrogen capacity. Most experiments to date produce hydrofullerides with a maximum of thirty-six bonded hydrogen atoms ($C_{60}H_{36}$), amounting to a storage density of 4.8 wt% hydrogen. In a few cases, $C_{60}H_{44}$ has been observed in mixtures with other, less-hydrogenated fullerenes,[20−22] and, very rarely, the presence of a trace of $C_{60}H_{52}$ (6.7 wt %) has been reported.[23] A second problem is the poor efficiency of charge and discharge, which is related to the energetics of the hydrogen bonding: When x in $C_{60}H_x$ is less than 36, the H atoms are too strongly bound to be retrieved efficiently, whereas at $x > 36$ the binding is too weak due to the strain associated with introduction of sp^3 bonding. Thus, there is both a high energetic cost to liberate hydrogen at low x and a high energetic cost to stabilize hydrogen at high x. Together, these factors lead to poor charge/discharge energy efficiency. Both reversible[20,24] and irreversible[25] hydrogenation/dehydrogenation reactions have been reported.

We show here that the use of an endohedral dopant circumvents these problems and that the internal metal−carbon interactions enable the coverage-dependent H binding to be a smoother and more desirable function of the H/C ratio. At lower H densities, the C−H binding is weakened by endohedral doping; however, at higher H densities ($x > 36$), the endohedral dopants strengthen the binding. As a result, the total H capacity is also increased. We investigate the hydrogenation of C_{60}, M@C_{60}, and M_2@C_{60} for M = Li, Be, Mg, Ca, Al, and Sc and compare how the encapsulated metals and the number of valence electrons (1−3) affect fullerene hydrogenation.

2. Computational Details

Since many hydrogenation pathways are possible, we focused on two model pathways (vide infra) thar cover a few rationally selected x values.[27] The reactions were divided into intervals from $C_{60}H_x$ to $C_{60}H_{x+m}$ and characterized by the interval-specific average binding energy for addition of H_2,

$$f = [E^{\mathrm{tot}}(C_{60}H_x) + (m/2)\mu(H_2) - E^{\mathrm{tot}}(C_{60}H_{x+m})]/(m/2) \qquad (1)$$

where E^{tot} is the total energy of the molecules in the parentheses. For simplicity, the hydrogen chemical potential, $\mu(H_2)$, was chosen to be the energy of a free hydrogen molecule. The zero-point energy, entropy, and H_2 pressure contributions are considered as constants here. This is a very rough approximation, which should be restricted to energetics discussions. For more accurate calculation of entropy, one must evaluate the contribution from the phonons (or vibration) of all the fullerene, hydrofulleride, and hydrogen molecules associated with their internal degree of freedom. By our definition, positive values of f mean energetically favorable binding.

We use spin-polarized first-principles method implanted in the Vienna Ab Initio Simulation Package.[28] A plane-wave basis set (400 eV cutoff) is used in combination with an all-electron-like projector augmented-wave potential and Perdew−Burke−Ernserhof exchange-correlation functional[29] within generalized

* Corresponding author. E-mail: yufeng_zhao@nrel.gov.
† National Renewable Energy Laboratory.
‡ Virginia Polytechnic Institute and State University.

10.1021/jp073482a CCC: $37.00
Published on Web 08/15/2007

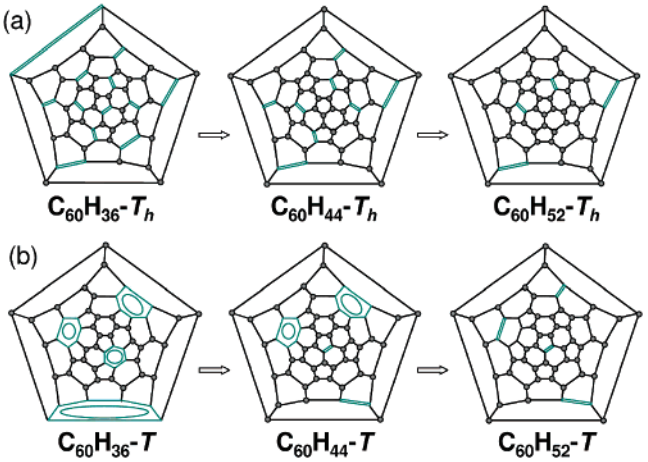

Figure 1. Two possible reaction pathways to hydrogenation of C_{60}, represented in Schlegel diagrams. The dots are hydrogenated carbon atoms. Double lines show the double bonds in the naked C pairs, and the ovals indicate the local aromatic rings. The marked symmetry for $C_{60}H_{44}$ and $C_{60}H_{52}$ are not strict but are for classification of the reaction pathways.

gradient approximations. In a periodic boundary condition, the cubic unit cell size in our calculations has a dimension of 25 Å to maintain sufficient vacuum surrounding the molecules.

3. Results and Discussions

In correspondence with previous studies on hydrogenation of pure fullerenes, we selected $x = 0$, 36, 44, and 52 for the $C_{60}H_x$'s along the H_2 addition pathway. Isomers of the different $C_{60}H_x$'s give different reaction pathways. For example, the $C_{60}H_{36}$ compound, the most studied hydrofulleride, has $\sim 10^{14}$ possible isomers.[30] Of these, the T_h structure (in Figure 1a) initially proposed by Haufler et al.[1] was later found to be a high-energy isomer,[30−37] while the T structure (in Figure 1b) predicted by Taylor[33] was found to be the ground state. These two well-known isomers highlight two different isomerization rules. In the T_h structure, all the unhydrogenated ("naked") carbon atoms form pairs, but these carbon pairs are isolated and evenly distributed across the hydrofulleride molecule to release the maximum strain. In contrast, in the T structure, the naked carbon pairs form aromatic rings, which are then evenly distributed throughout the cage. Although energetically more favorable, the aromatic rings may not be formed with an approach such as the Birch reduction, since only conjugated double bonds are attacked. Consequently, experimentalists find diverse $C_{60}H_{36}$ isomers in their products,[19,38,39] with the T structure being quite rare.[34,40] This suggests that the hydrogenation reaction pathway is mostly determined by kinetics rather than by minimum energy considerations. Our calculations show that the T_h structure of $C_{60}H_{36}$ is 3.0 eV above its T isomer and that a C_3 isomer has the second-lowest energy (0.2 eV above the T isomer), in good agreement with previous calculations.[19,31,32,36,37] Here we studied two model reaction pathways following the above two rules of isomerization, with the higher energy pathway traveling through the $C_{60}H_{36}$-T_h and the low-energy one passing through $C_{60}H_{36}$-T. Between C_{60} and $C_{60}H_{36}$, other hydrofullerides, e.g., $C_{60}H_2$ and $C_{60}H_{18}$-C_{3v} (with aromatic rings), were also observed.[18,41] Our calculation gives binding energies of 0.904, 1.080, and 0.950 eV/H_2 as average energies for hydrogenation over the intervals $C_{60} \rightarrow C_{60}H_2$, $C_{60}H_2 \rightarrow C_{60}H_{18}$-$C_{3v}$, and $C_{60}H_{18}$-$C_{3v} \rightarrow C_{60}H_{36}$-$T$, respectively. This indicates that the energy landscape for the addition of H is largely featureless until $C_{60}H_{36}$, which is also true for the high-energy pathway. Previous calculations[42] also show that the strain becomes critically minimized at $C_{60}H_{36}$. Consequently, we find no need to study additional x values between 1 and 36.

TABLE 1: Average Binding Energies (in eV/H_2) in Different Stages of Fullerene Hydrogenation in Path-T_h

	$C_{60} \rightarrow C_{60}H_{36}$	$C_{60}H_{36} \rightarrow C_{60}H_{44}$	$C_{60}H_{44} \rightarrow C_{60}H_{52}$
C_{60}	0.880	0.426	0.095
Li@C_{60}	0.840	0.543	0.260
Li_2@C_{60}	0.711	0.562	0.311
Mg_2@C_{60}	0.708	0.513	0.382
Ca@C_{60}	0.782	0.561	0.130
Ca_2@C_{60}	0.660	0.582	0.335
Al_2@C_{60}	0.785	0.776	0.448

Very little is known about the structures of the more highly hydrogenated fullerenes such as $C_{60}H_{44}$ and $C_{60}H_{52}$. Here, we computationally search for stable isomers guided by the same rules for the two reaction paths. Having investigated over 100 $C_{60}H_{44}$ isomers, we have found that these two rules work well, predicting here the lowest-energy $C_{60}H_{44}$-T isomer (in Figure 1b). This is because the two naked carbon pairs (double bonded) are equidistant between the two aromatic rings, which release the maximum strain. For the same reasons, we find $C_{60}H_{52}$-T (in Figure 1b) to be the lowest energy isomer by adding four H's to every one of the four aromatic rings in the $C_{60}H_{36}$-T structure, which leaves four equilaterally located, naked carbon pairs. The sequences in Figure 1 are considered as two reaction paths (denoted as path-T_h and path-T) starting from C_{60}, because the isomers of $C_{60}H_{44}$ and $C_{60}H_{52}$ in parts a and b are results of direct H addition to the $C_{60}H_{36}$-T_h and -T isomers, respectively. Now the key question is: How do endohedral dopants affect the corresponding reaction behavior?

Table 1 gives the average hydrogenation energies encountered along path-T_h (Figure 1a). A first thing to note is that the formation energy of $C_{60}H_{36}$ is reduced by up to 0.2 eV/H_2 when metals are inside, as shown in Figure 2. Second, incorporation of an endohedral metal increases the formation energies of $C_{60}H_{44}$ and $C_{60}H_{52}$. Without the endohedral metal atom, hydrogen is very weakly bound in the range between $C_{60}H_{44}$ and $C_{60}H_{52}$, while endohedral doping increases H binding by as much as a factor of 4. Thus the first 36 H atoms are easier to retrieve, and the later 8 H atoms are easier to load. Importantly, we find a correlation between the binding energy changes and the electronegativity and number of valence electrons of the metal atom. Qualitatively, the lower the electronegativity and the more valence electrons in the corresponding metal atoms, the larger the change in the H binding energy relative to the pure C_{60} case. This implies that charge transfer from the metal to the fullerene cage plays an important role.[43,44]

The corresponding reaction behavior for path-T (Figure 1b) is summarized in Table 2. It is not surprising that this path ends with $C_{60}H_{36}$-T, a tetrahedron with four aromatic rings on the flat faces and carbon hydrides along the bent edges. This is an ideal structure in which aromaticity and strain relief considerations are synchronously satisfied. The addition of a single additional dihydride unit harms both. Without doping, neither $C_{60}H_{44}$-T nor $C_{60}H_{52}$-T is energetically favorable relative to $C_{60}H_{36}$-T, which has a formation energy as high as 1.05 eV/H_2 (Table 2). Again, the endohedral doping weakens H binding in $C_{60}H_{36}$-T by up to 0.2 eV/H_2 yet permits hydrogenation to $C_{60}H_{44}$-T for all dopants. Hydrogenation to $C_{60}H_{52}$-T is now possible with endohedral Be, Mg, and Ca, although the compounds are not as stable as in the T_h case. However, it is

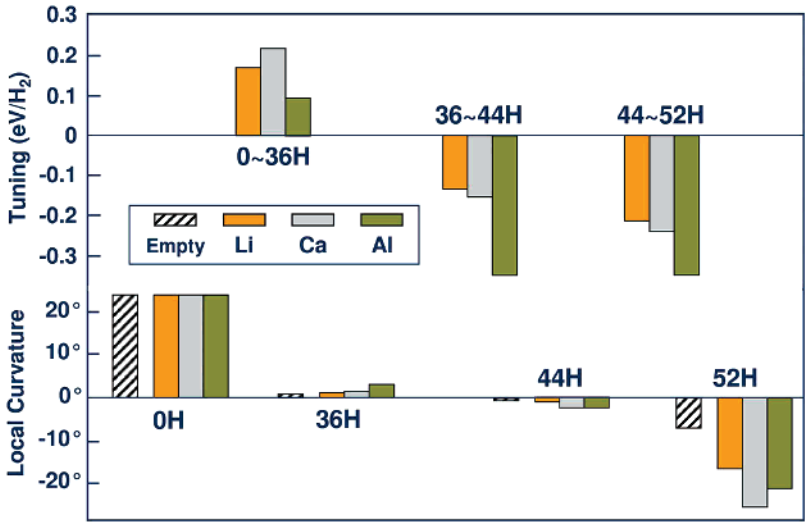

Figure 2. (Up) Tuning behavior in path-T_h measured by reduction of H binding energies due to doping of the cage with two Li, Ca, and Al atoms. Positive means binding weakening, and negative indicates binding enhancement. (Down) Local curvature averaged over all double bonds (naked carbon pairs) in the molecule $C_{60}H_x$-T_h or $M_2@C_{60}H_x$-T_h, where $x = 36$, 44, and 52, compared to the unhydrogenated fullerenes. The local curvature is measured by the summation of the three bond angles around a carbon atom subtracted by 360°, with the negative (positive) value indicating inward (outward) curvature.

TABLE 2: Average Binding Energies (in eV/H_2) in Different Stages of Fullerene Hydrogenation in Path-*T*

	$C_{60} \rightarrow C_{60}H_{36}$	$C_{60}H_{36} \rightarrow C_{60}H_{44}$	$C_{60}H_{44} \rightarrow C_{60}H_{52}$
C_{60}	1.046	−0.104	−0.078
$Li_2@C_{60}$	0.947	0.068	−0.067
$Be_2@C_{60}$	0.981	0.303	0.006
$Mg_2@C_{60}$	0.866	0.067	0.080
$Ca_2@C_{60}$	0.801	0.150	0.050
$Al_2@C_{60}$	0.917	0.704	−0.002
$Sc_2@C_{60}$	0.858	0.160	−0.179

clear that the binding-energy tunability is a general trend independent of the reaction path.

The binding energy reduction for the first 36 hydrogen atoms (see Figure 2 for path-T_h) can be understood in terms of charge transfer. The C_{60} fullerene has high electronegativity[42] due to the low LUMO level and forms a more stable complex with encapsulated metals atoms. This chemically inert complex is thus more difficult to hydrogenate as compared with pure C_{60}, whose LUMO level will be pushed up by hydrogenation. As it will be described in details below, the LUMO level of $C_{60}H_x$ steadily goes up with the hydrogen coverage increases but stops at some intermediate value, $36 < x < 44$, and then starts to drop at high coverage due to a new factor, i.e., negative (inward) curvature induced by strain. An examination of the atomic structure of $C_{60}H_{52}$-T_h, shows that over-hydrogenation tends to introduce local negative curvature in the naked sites to release the strain. This weakens the π bonds, creating some component of inward sp^3-like dangling bonds in the "naked" carbon pairs, pushing the bonding states (HOMO) up and pulling down the antibonding states (LUMO). Thus, a high H density in empty hydrofullerides is energetically unfavorable. However, with metals inside, both the LUMO and HOMO states (localized at these negatively curved sites) hybridize with the metal atoms, which stabilizes the negative curvature. We will see that the carbon−metal hybridization can be in the form of either charge transfer or bonding, depending on the metal atoms. The local curvature shown in Figure 2 is measured by the summation of three bond angles around a naked carbon atom subtracted by 360°, and the negative (positive) value denotes inward (outward) curvature. It is seen that negative curvature begins to occur in $C_{60}H_{44}$ and becomes significant in $C_{60}H_{52}$. The endohedral

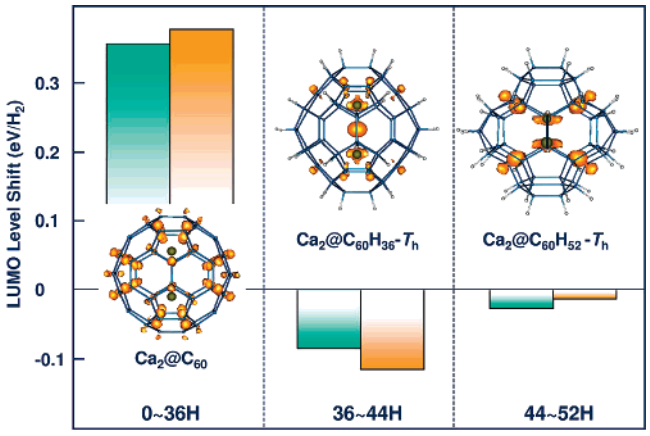

Figure 3. Energy shift summation over the two lowest-unoccupied molecular orbitals (LUMO) per H_2 addition in different stages of hydrogenation of empty C_{60}. Green and orange bars are respectively for T_h and T paths. It is seen that from C_{60} to $C_{60}H_{36}$, the LUMO levels are lifted up by over 0.3 eV per H_2. With further increase of H coverage, the LUMO levels drops. Once metal atoms are encapsulated, the charge transfer from metal to the cage decreases in $Ca_2@C_{60}H_{36}$-T_h and then increases again in $Ca_2@C_{60}H_{52}$-T_h, as is shown by the insets, where the charge density is contributed by the four electrons just below the Fermi level.

dopants enhance the negative curvature, indicating hybridization between the naked carbon and the metal atoms.

Figure 3 shows the details of hydrogenation-induced energy shift of the LUMO states of the empty cages and the electron-density distribution upon metal encapsulation for path-T_h. In $Ca_2@C_{60}$, for example, most of the valence electrons of the two Ca atoms are transferred to the cage, whereas only fractional charge is transferred from the Ca−Ca bond in the case of $Ca_2@C_{60}H_{36}$-T_h. But the negatively curved carbon sties in $Ca_2@C_{60}H_{52}$-T_h attract more charge from the Ca atoms, leaving little electron density on the Ca−Ca bond. In the case of Al (and Be), due to its larger electronegativity, we observe that strong bonds with the C atoms pull the C atoms further inward and enhance the negatively curved sites (Figure 4). A third factor comes into play when transition-metal Sc atoms are used as dopants. The transition metal atoms interact strongly with both the π bonds and the low-lying empty π^* orbitals in the cages

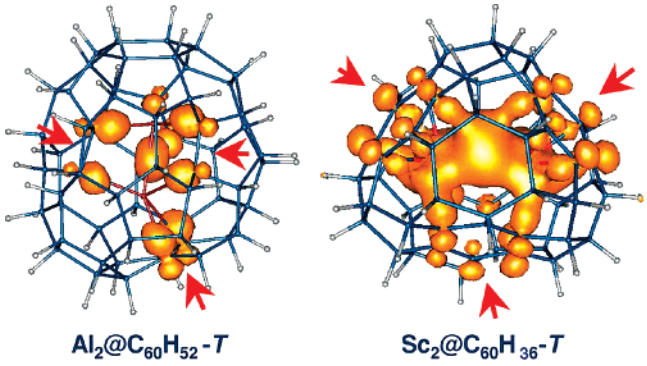

Figure 4. Charge density contributed by six electrons below the Fermi level. In $Al_2@C_{60}H_{52}$-*T*, the naked carbon pairs (red arrows) are pulled inward to form bonds with Al atoms. In $Sc_2@C_{60}H_{36}$-*T*, the Sc atoms coordinate with the aromatic rings (red arrows) in the cage.

through Dewar coordination.[45,46] This explains the relative smaller reduction of the formation energy of $Sc_2@C_{60}H_{36}$-*T* and the larger reduction of those of $Sc_2@C_{60}H_{44}$ and $Sc_2@C_{60}H_{52}$, because the four aromatic rings in $C_{60}H_{36}$-*T* interact strongly with Sc atoms, as shown in Figure 4.

Importantly, the hydrogenation/dehydrogenation process appears to be completely reversible. Once the hydrogen atoms are removed, the metal−carbon bonds break, and a spherical fullerene cage is spontaneously recovered. This agrees with the experimentally demonstrated reversibility.[20,24] One main concern associated with the reversibility is that fullerene reaction may occur during hydrogenation at high temperature.[25] Fortunately, the endohedral metallofullerenes are chemically more stable than pure fullerenes due to the complexing of the interior of the fullerene by the encapsulated metals.[47] Therefore, using endohedral dopants would improve the reversibility. Also, the barriers for hydrogen dissociation and dehydrogenation will be important parameters for the kinetics and the reversibility. According to our constraint-dynamics calculation, the encapsulated metals, at least for the specific case of $Ca_2@C_{60}$, cannot reduce the reaction barrier. The dehydrogenation barriers are 3.8 and 3.9 eV, respectively, for $Ca_2@C_{60}H_2$ and empty $C_{60}H_2$, in which the hydrogen atoms are initially attached to the two ends of a double C−C bond. The barriers of the reverse process, i.e., H_2 dissociation, are 3.2 and 3.1 eV, respectively. Technically, the high barriers should not be a major problem because external catalysts may be employed.

The encapsulated metals change the thermodynamics and will therefore undoubtedly change the dynamics associated with the isomerization. For example, we can surmise that some isomers may be stabilized and that the reaction paths may be altered. This would be an interesting topic, but a detailed investigation must be saved for future work. In any case, the tuning behavior of the binding energy is clear.

The use of larger fullerene cages such as C_{70} or C_{80} would further reduce the upper limit of H-binding energy. Interestingly, a recent computational study[48] of the *i*-$Sc_3N@C_{80}H_x$ also shows substantial binding energy reduction (from ~1.1 to 0.65 eV/H_2; see Figure 3 therein) at lower H coverage ($x < 44$) due to the encapsulated Sc_3N cluster, which strongly supports our theory. Because sequential binding energies were not calculated in ref 48, it is not clear how the H-binding strength changes at higher coverage. However, the fact that the average binding energy in *i*-$Sc_3N@C_{80}H_x$ decreases less fast than that in *i*-$C_{80}H_x$ as x approaches 72 may imply an enhanced H binding in the high coverage region in *i*-$Sc_3N@C_{80}H_x$. Therefore, our theory is applicable to *i*-$Sc_3N@C_{80}$, indicating that the tuning behavior we proposed here is universal for all endohedral metallofullerenes.

4. Conclusion

In summary, we have demonstrated that endohedral metallofullerenes can behave as tunable hydrogen-storage materials. The desirable tuning of the hydrogen-binding energies and capacities occurs naturally through interplay between charge transfer and bond rehybridization effects. At lower H densities, when H atoms are too strongly bound to pure C_{60}, the endohedral dopants weaken the binding. The dopants also enhance the hydrogen-binding energy at higher coverage and enable the degree of hydrogenation to be substantially increased relative to that available with empty-cage C_{60}. Overall, the encapsulated metals increase the capacity and improve the energy efficiency for hydrogen storage. These studies point to the possible use of endohedral metallofullerenes for hydrogen storage and highlight key physical and chemical principles that may be harnessed to design future materials with even better properties. From a fundamental viewpoint, this study demonstrates an unconventional catalysis. Unlike the conventional catalysts, which contact with both reactants and reduce the reaction barrier of a single-step reaction, the catalyst here is hidden in one of the reactants but systematically modifies the dynamics of the complicated, sequential reaction process. This study shows vividly the interplay between the "inside chemistry" and "outside chemistry" as was envisioned in ref 1 for fullerenes.

Acknowledgment. This work is supported by DOE Office of Science, Basic Energy Sciences, Division of Materials Science, and the Office of Energy Efficiency and Renewable Energy Hydrogen through the Center of Excellence for Carbon Based Materials for Hydrogen Storage.

References and Notes

(1) Haufler, R. E.; Conceicao, J.; Chibante, L. P. F.; Chai, Y.; Byrne, N. E.; Flanagan, S.; Haley, M. M.; Obrien, S. C.; Pan, C.; Xiao, Z.; Billups, W. E.; Ciufolini, M. A.; Hauge, R. H.; Margrave, J. L.; Wilson, L. J.; Curl, R. F.; Smalley, R. E. *J. Phys. Chem.* **1990**, *94*, 8634−8636.

(2) Bethune, D. S.; Johnson, R. D.; Salem, J. R.; Devries, M. S.; Yannoni, C. S. *Nature* **1993**, *366*, 123−128.

(3) Akasaka, T.; Nagase, S. Endofullerenes: *A New Family of Carbon Cluster*; Kluwer Academic Publishers: Dordrecht, 2002.

(4) Shinohara, H. *Rep. Prog. Phys.* **2000**, *63*, 843−892.

(5) Wilson, L. J.; Cagle, D. W.; Thrash, T. P.; Kennel, S. J.; Mirzadeh, S.; Alford, J. M.; Ehrhardt, G. J. *Coord. Chem. Rec.* **1999**, *190*−*192*, 199−207.

(6) Sun, D.; Liu, Z.; Guo, X.; Xu, W.; Liu, S. *Fullerene Sci. Technol.* **1997**, *5*, 137−143.

(7) Gu, G.; Huang, H. J.; Yang, S. H.; Yu, P.; Fu, J. S.; Wong, G. K.; Wan, X. G.; Dong, J. M.; Du, Y. W. *Chem. Phys. Lett.* **1998**, *289*, 167−173.

(8) Hino, S.; Umishita, K.; Iwasaki, K.; Miyazaki, T.; Miyamae, T.; Kikuchi, K.; Achiba, Y. *Chem. Phys. Lett.* **1997**, *281*, 115−122.

(9) Grannan, S. M.; Birmingham, J. T.; Richards, P. L.; Bethune, D. S.; De Vries, M. S.; Van Loosdrecht, P. H. M.; Dorn, H. C.; Burbank, P.; Bailey, J.; Stevenson, S. *Chem. Phys. Lett.* **1997**, *264*, 359−365.

(10) Ding, X. Y.; Aldord, J. M.; Wright, J. C. *Chem. Phys. Lett.* **1997**, *269*, 72−78.

(11) Ding, J. Q.; Yang, S. H. *Angew. Chem. Int. Ed.* **1996**, *35*, 2234−2235.

(12) Okazaki, T.; Lian, Y.; Gu, Z.; Suenaga, K.; Shinohara, H. *Chem. Phys. Lett.* **2000**, *320*, 435−440.

(13) Cai, T.; Xu, L. S.; Anderson, M. R.; Ge, Z. X.; Zuo, T. M.; Wang, X. L.; Olmstead, M. M.; Balch, A. L.; Gibson, H. W.; Dorn, H. C. *J. Am. Chem. Soc.* **2006**, *128*, 8581−8589.

(14) Stevenson, S.; Rice, G.; Glass, T.; Harich, K.; Cromer, F.; Jordan, M. R.; Craft, J.; Hadju, E.; Bible, R.; Olmstead, M. M.; Maitra, K.; Fisher, A. J.; Balch, A. L.; Dorn, H. C. *Nature* **1999**, *401*, 55−57.

(15) Nossal, J.; Saini, R. K.; Alemany, L. B.; Meier, M.; Billups, W. E. *Eur. J. Org. Chem.* **2001**, 4167−4180.

(16) Scuseria, G. E. *Chem. Phys. Lett.* **1991**, *176*, 423−427; Cioslowski, J. *Ibid*. 1**991**, *181*, 68−72.
(17) Matsuzawa, N.; Dixon, D. A.; Fukunaga, T. *J. Phys. Chem.* **1992**, *96*, 7594−7604.
(18) Henderson, C. C.; Cahill, P. A. *Science* **1993**, *259*, 1885−1887.
(19) Nossal, J.; Saini, R. K.; Sadana, A. K.; Bettinger, H. F.; Alemany, L. B.; Scuseria, G. E.; Billups, W. E.; Saunders, M.; Khong, A.; Weisemann, R. *J. Am. Chem. Soc.* **2001**, *123*, 8482−8495.
(20) Darwish, A. D.; Abdulsada, A. K.; Langley, G. J.; Kroto, H. W.; Taylor, R.; Walton, D. R. M. *J. Chem. Soc. Perkin Trans.* **1995**, *2*, 2359−2365.
(21) Peera, A. A.; Alemany, L. B.; Billups, W. E. *Appl. Phys. A* **2004**, *78*, 995−1000.
(22) Shigematsu, K.; Abe, K.; Mitani, M.; Tanaka, K. *Fullerene Sci. Technol.* **1993**, *1*, 309−31.
(23) Darwish, A. D.; Taylor, R.; Loutfy, R. *Fullerenes* 2000−Volume 9*: Functionalized Fullerenes;* Electrochem. Soc. Proc. Vol. 2000−11, p 179.
(24) Withers, J. C.; Loutfy, R. O.; Lowe, T. P. *Fullerene Sci. Technol.* **1997**, *5*, 1−31.
(25) Brosha, E. L.; Davey, J.; Garzon, F. H.; Gottesfeld, S. *J. Mater. Res.* **1999**, *14*, 2138−2146.
(26) Wang, N.-X.; Zhang, J.-P. *J. Phys. Chem. A* **2006**, *110*, 6276−6278.
(27) Fullerene hydrogenation is a one-by-one addition of H atoms to the C-cage, involving a complicated evolution of the nanostructures. [see Zhao, Y.; et al. *Phys. Rev. Lett.* **2002**, *88*, 185501; *Phys. Rev. B.* **2002**, *66*, 195409.] Determination of the minimum energy path (MEP) by max($\sum_n f_n$), where f_n is the absolute value of the formation energy or binding energy of the *n*th H atom, is not feasible because it requires surveying countless combinations of all $C_{60}H_x$ isomers over $0 < x < 60$. Also, in reality, a reaction goes through multiple channels, unnecessarily depending on the MEP.
(28) Kresse, G.; Furthmüller, J. *Phys. Rev. B* **1996**, *54*, 11169−11186.
(29) Perdew, J. P.; et al. *Phys. Rev. B* **1992**, *46*, 6671; Perdew, J. P.; Burke, K.; Ernzerhof, M. *Phys. Rev. Lett.* **1996**, *77*, 3865−3868.
(30) Balasubramanian, K. *Chem. Phys. Lett.* **1991**, *182*, 257−262.
(31) Clare, B. W.; Kepert, D. L. *J. Mol. Struct.* (*THEOCHEM*) **1994**, *303*, 1−9; *Ibid*. **1994**, *304*, 181−189; *Ibid*. **1994**, *315*, 71−83; *Ibid*. **1999**, *466*, 177−186.
(32) Buhl, M.; Thiel, J. W.; Schneiders, U. *J. Am. Chem. Soc.* **1995**, *117*, 4623−4627.
(33) Taylor, R. *J. Chem. Soc. Perkin Trans.* **1992**, *2*, 1667−1669.
(34) Austin, S. J.; Batten, R. C.; Fowler, P. W.; Redmond, D. B.; Taylor, R. *J. Chem. Soc., Perkin Trans.* **1993**, *2*, 1383−1386.
(35) Rathna, A.; Chandrasekhar, J. *Chem. Phys. Lett.* **1993**, *206*, 217−224.
(36) Dunlap, B. I.; Brenner, D. W.; Schriver, G. W. *J. Phys. Chem.* **1994**, *98*, 1756−1757.
(37) Book, L. D.; Scuseria, G. E. *J. Phys. Chem.* **1994**, *98*, 4283−4286.
(38) Bensasson, R. V.; Hill, T. J.; Land, E. J.; Leach, S.; McGarvey, D. J.; Truscott, T. G.; Ebenhoch, J.; Gerst, M.; Ruchardt, C. *Chem. Phys.* **1997**, *215*, 111−123.
(39) Bini, R.; Ebenhoch, J.; Fanti, M.; Fowler, P. W.; Leach, S.; Orlandi, G.; Ruchardt, C.; Sandall, J. P. B.; Zerbetto, F. *Chem. Phys.* **1998**, *232*, 75−94.
(40) Boltalina, O. V.; Buhl, M.; Khong, A.; Saunders, M.; Street, J. M.; Taylor, R. *J. Chem. Soc. Perkin Trans.* **1999**, *2*, 1475−1479.
(41) Darwish, A. D.; Avent, A. G.; Taylor, R.; Walton, D. R. M. *J. Chem. Soc. Perkin Trans.* **1996**, *2*, 2051−2054.
(42) Yoshida, Z.; Dogane, I.; Ikehira, H.; Endo, T. *Chem. Phys. Lett.* **1992**, *201*, 481−484.
(43) Kobayashi, K.; Nagase, S. *Chem. Phys. Lett.* **1996**, *262*, 227−232.
(44) Aihara, J. *Chem. Phys. Lett.* **2001**, *343*, 465−469.
(45) Mingos, D. M. P. *J. Organomet. Chem.* **2001**, *635*, 1−8.
(46) Zhao, Y.; Dillon, A. C.; Kim, Y.-H.; Heben, M. J.; Zhang, S. B. *Chem. Phys. Lett.* **2006**, *425*, 273−277.
(47) Fowler, P. W.; Zerbetto, F. *Chem. Phys. Lett.* **1995**, *243*, 36−41.
(48) Campanera, J. M.; Heggie, M. I.; Taylor, R. *J. Phys. Chem. B* **2005**, *109*, 4024−4031.